International Journal of Control

ISSN: (Print) (Online) Journal homepage: https://www.tandfonline.com/loi/tcon20

An improved U-control design for nonlinear systems represented by input/output differential models with a disturbance observer

Ruobing Li, Quanmin Zhu, Weicun Zhang, Xicia Yue & Pritesh Narayan

To cite this article: Ruobing Li, Quanmin Zhu, Weicun Zhang, Xicia Yue & Pritesh Narayan (2023) An improved U-control design for nonlinear systems represented by input/output differential models with a disturbance observer, International Journal of Control, 96:11, 2737-2748, DOI: 10.1080/00207179.2022.2111370

To link to this article: https://doi.org/10.1080/00207179.2022.2111370

Published online: 18 Aug 2022.

INTERNATIONAL JOURNAL OF CONTROL
2023, VOL. 96, NO. 11, 2737–2748
https://doi.org/10.1080/00207179.2022.2111370

An improved U-control design for nonlinear systems represented by input/output differential models with a disturbance observer

Ruobing Li[a], Quanmin Zhu[a], Weicun Zhang[b], Xicia Yue[a] and Pritesh Narayan[a]

[a]Department of Engineering Design and Mathematics, University of the West of England, Bristol, UK; [b]School of Automation and Electrical Engineering, University of Science and Technology Beijing, Beijing, People's Republic of China

ABSTRACT

This paper presents a new method to calculate the inversion of the controlled linear/nonlinear dynamic plants which are described by input–output differential equation models. This new U-model-based inverter (U-inverter), cancels both system dynamics and nonlinearities, can be used directly to facilitate the control system design, which the design of U-model-based control (U-control) systems is selected for demonstration in this study. The most important advantage of this U-inverter is that it does not require system state variables, only uses the input/output measurements from the controlled plants. A nonlinear disturbance observer is introduced into the U-control design framework to increase its robustness. The analysis explains the properties of this developed the disturbance observer-based U-control (DOBUC) method and its design procedures. Finally, a wind energy conversion system is simulated to illustrate the design of this DOBUC and the corresponding performance.

ARTICLE HISTORY
Received 15 April 2022
Accepted 2 August 2022

KEYWORDS
U-model based control (U-control); disturbance observer (DOB); dynamic inversion; wind energy conversion system (WECS)

1. Introduction

The discrepancies between the real-time controlled applications and their mathematical modelling are always one of the main problems in the control system design. These discrepancies include system external disturbances and internal modelling errors which can result in critically pernicious effects on engineering practical operations and research development. There are at least two ways to deal with these control design problems caused by mentioned discrepancies. The first one involves robust control which considers the worst-case situation in the control system design and uses feedback principium to suppress the uncertainties and disturbances (Ding et al., 2020; Shen et al., 2018; Wang et al., 2022). However, this kind of methods may over-estimate the upper disturbances' bounds and therefore results in unsatisfactory system dynamic and control performance. The second approach is based on discrepancies estimation and compensation theory. Generally, this kind of composite control system (Zhang et al., 2018) contains two design steps: design a baseline controller to meet the required control performance in the external loop and a disturbance attenuator to cancel or compensate the discrepancies in an inner loop. In the approach considered in this study, a disturbance observer (DOB) is used for discrepancies estimation between the real-time controlled plant and its mathematical modelling.

The accurate estimation of system uncertainties and disturbances is compulsory and required in DOB-based control (DOBC) design. The fundamental DOB structure in the frequency-domain was first proposed in 1980s (Ohishi et al., 1987), which estimates the lumped system disturbances by using the dissimilarity between the control system input measurement and the theoretical input calculated by the controlled plant's dynamic inversion. Accordingly, the basic principle of this DOB (Ohishi et al., 1987) is to amalgamate all uncertainties and system external disturbances into the control input channel. Remarkably, this frequency-domain DOB is applicable for linear control systems, or nonlinear control systems that consider nonlinearity as uncertainty. However, for some nonlinear control systems, the estimation performance by this linear frequency-domain DOB may not be satisfactory in practical operations. Generally, dynamic modelling of many practical nonlinear systems has been well understood and applied, the variables of which are also measurable with high accuracy (Chen et al., 2016), therefore, making extensive assumptions about unknown elements subject to mild constraints, the cautiously reasonably using of such available information/assumptions could promote more efficient control system design.

To deal with nonlinearities efficiently, nonlinear DOB (NDOB) was first proposed by (Chen et al., 2000) based on the estimation of disturbance torque caused by a disturbance in robotic manipulators. In a work (Chen, 2003), Lyapunov stability theory and mathematical analysis proved that the perturbation error estimated by the NDOB method will exponentially converge to zero. Based on these theoretical analysis and proof, the NDOB method has been widely used in academic research and many real-time applications, such as UAV attitude control design (Chen et al., 2020), position control of seven-degree-of-freedom nonlinear manipulators (Müller et al., 2020), Quadrotor complex attitude tracking control (Ahmed et al., 2020).

CONTACT Ruobing Li ruobing2.li@live.uwe.ac.uk Department of Engineering Design and Mathematics, University of the West of England, Frenchy Campus, Coldharbour Lane, Bristol BS16 1QY, UK

Another method, which develops the linear frequency-domain DOBC to be applied to a nonlinear system (Li, Zhu, Yang, et al., 2021), involves nonlinear inversion calculated by the U-model-based dynamic inversion method (Li et al., 2020). Compared with (Chen et al., 2000) both assume that the state variables are gauged, and the DOB in Li, Zhu, Yang, et al. (2021) can amalgamate all the uncertainties and external system disturbances into a control input channel, which is more intuitional and can be used for system input compensation directly with less computation and simpler adjustment (Li, Zhu, Yang, et al., 2021). However, the DOB design in Li, Zhu, Yang, et al. (2021) only focuses on a fully actuated system and requires the high-order derivative of system output or state variables, which restricts its practical applications.

Another component of the DOBC is a baseline controller that meets the required specifications of control system performance. Based on the principles of the U-model control (U-control) (Zhang et al., 2020; Zhu et al., 2015), the controlled plant can be recompensed to a unit constant or identity matrix through UM dynamic inversion method (Li et al., 2020), therefore cancelling the system dynamic and nonlinearity simultaneously, providing a control system design method with no phase delay between system input and output. Therefore, the superiority of U-control has attracted research. For example, U-neuro-control (Zhu, Zhang, Zhang, et al., 2019), U-internal model control (Hussain et al., 2019), U-two-degree-of-freedom IMC (Li, Zhu, Narayan, et al., 2021) and U-double-sliding-model control (Zhu et al., 2022). However, the approaches in Hussain et al. (2019), Li, Zhu, Narayan, et al. (2021), Zhang et al. (2020), Zhu et al. (2015, 2022) and Zhu, Zhang, Zhang, et al. (2019) require system state variables to be known or measurable, in other words, if certain system state variables are unmeasurable or difficult to measure, these control methods cannot be applied or cost expensively. (Zhu, 2021) applies an Extend State Observer (ESO) to observe state variables and uses the observed state variables to design a controller, but the limitations of ESO restrict its practical applications. Inspired by this significant research, the purpose of this study is to develop a novel U-control design framework that only uses the input/output signal from the control system. Additionally, because of the high sensitivity of the U-inverter to the system modelling and system external disturbances, the proposed U-control design framework is combined with a nonlinear DOB (Ding et al., 2019) which also only requires the input/output measurements from the control system to increase its robustness.

Summarily, the main contributions in this paper are: Firstly, a new U-control design framework has been proposed with the utility of input/output measurement from the control system, which also provides a robust dynamic inversion scheme and can cancel both system dynamics and nonlinearities. Secondly, this study provides a universal phase delay-free, fast-response and convenient control system design framework through the integration of U-control and NDOB, which is acceptable to all linear/nonlinear control systems. The rest of the organization of this paper is: Section 2 presents the basic theory and assumption linking to the follow-up technology study. Section 3 proposes a novel disturbance observer-based U-control (DOBUC) design framework with convergence analysis through mathematics. A simulation experiment of control of wind energy conversion system (WECS) illustrates the feasibility and efficiency of the studies in Section 4. Finally, Section 5 concludes the whole findings in this study.

2. Problem statement

This study considers the following SISO input/output differential equation to describe a general nonlinear dynamic system

$$y_1^{(n)} = f(Y_1) + g_0(Y_1)u + \ldots + g_m(Y_1)u^{(m)},\ m \le n \tag{1}$$

where y_1 is the system output, u is the system input, Y_1 absorbs all the system output y_1 and its derivatives except the highest order one $y_1^{(n)}$, that is

$$Y_1 = (y_1, \dot{y}_1, \ddot{y}_1, \ldots, y_1^{(n-1)}) \tag{2}$$

Remark 2.1: Model (1) is widely used to describe a kind of flat nonlinear system (Conte et al., 2007). Generally, $g_i(Y_1) = 0, i \in \mathbb{N}^+$ applied in many practical applications, it means the high order derivatives of system input $u^{(i)}, i \in \mathbb{N}^+$ are not existed. When the system considers actuator, $g_i(Y_1) = 0, i \ge 2$, it means the control system only needs system input u and its derivative $\dot{u}$.

Assumption 2.1 (BIBO): *The system output y_1 and its related higher-order derivatives $\dot{y}_1, \ddot{y}_1, \ldots, y_1^{(n-1)}$ can be bounded with a proper control input u. That is, the bounded input and bounded output (BIBO).*

Assumption 2.2 (Invertibility): *The following zero dynamic meets globally asymptotically stability:*

$$g_0(Y_1)u + g_0(Y_1)\dot{u} + \ldots + g_m(Y_1)u^{(m)} = 0 \tag{3}$$

Remark 2.2: Assumption 2.1 has been well pre-requested by a lot of linear/nonlinear control systems with BIBO stability. Technically, this assumption would limit the field of applications with unstable zero dynamic plants. In this study, assumption 2.1 that 'the output y and its derivatives are bounded' is a reasonable assumption for practical BIBO systems. Surely in future studies, dealing with unstable dynamics is a challenging topic.

Meanwhile, the zero dynamics of system (1) is in case of

$$g_0(0)u + g_0(0)\dot{u} + \ldots + g_m(0)u^{(m)} = 0 \tag{4}$$

The dynamic system (4) is globally asymptotically stable when it satisfies Assumption 2.2, which means the control system described in (1) is minimum-phase/linear plants or stable zero dynamics/nonlinear plants. When using (1) to describe linear dynamic systems, it turns to:

$$\begin{aligned} y_1^{(n)} + a_{n-1}y_1^{(n-1)} + \ldots + a_1\dot{y}_1 + a_0y_1 \\ = b_mu^{(m)} + b_{m-1}u^{(m-1)} + \ldots + b_0\dot{u} + b_0u,\ m \le n \end{aligned} \tag{5}$$

Then Assumption 2.2 turns to:

$$b_mu^{(m)} + b_{m-1}u^{(m-1)} + \ldots + b_0\dot{u} + b_0u = 0 \tag{6}$$

which directly links to the property of stable zero dynamics for the control system (5). The next step is to use the U-control

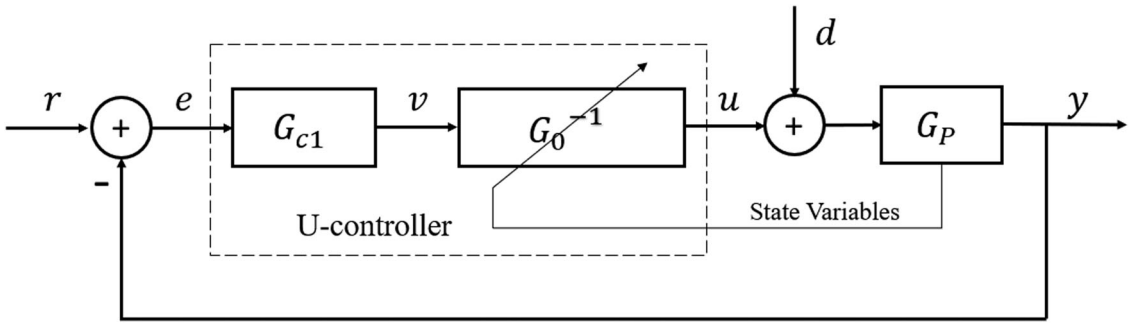

Figure 1. U-control system design framework.

method to design the baseline controller to cancel both the nonlinearity and dynamic of (1) and design a DOB to improve its robustness. It should be mentioned that all design of this new composite control system only uses the measurement from the control input u and the output y of the system (1), rather than requiring other information like high-order derivatives of system output $y^{(n)}$ and/or system state variables.

3. New design DOBUC systems

3.1 U-model-based control design

The continues-time (CT) U-control system design framework is shown in Figure 1 (Zhu, Zhang, Na, et al., 2019). The U-control system separates the controlled plant inversion and baseline controller design in double feedback loops. The inner loop is controlled plant's dynamic inversion aiming to cancel system nonlinearities and dynamics (Zhu & Guo, 2002). Accordingly, the output of the U-control system can be expressed as

$$y = \frac{G_{c1}G_0^{-1}G_P}{1 + G_{c1}G_0^{-1}G_P}r + \frac{G_P}{1 + G_{c1}G_0^{-1}G_P}d \tag{7}$$

where G_{c1} is called the invariant controller, G_P is the practical controlled plant and G_0^{-1} is its nominal inversion. r is the reference tracking signal. Model $G_P = G_0$ can be attained when the control system is free of modelling errors and external disturbance, distinctively, the output of (7) can be simplified when $G_P = G_0$:

$$y = \frac{G_{c1}}{1 + G_{c1}}r = Gr \tag{8}$$

where G describes the total gain of this control system, which can be easily designed by customer-defined damping ratio ζ and undamped natural frequency ω_n typically.

According to the U-M inversion algorithm (Li et al., 2020), the inversion of system (1) is expressed as

$$\begin{aligned} G_P^{-1} \Leftrightarrow u^{(m)} \in\ & y_1^{(n)} - f(Y_1) - g_0(Y_1)u \\ & - \ldots - g_m(Y_1)u^{(m)} = 0, \quad m \le n \end{aligned} \tag{9}$$

Remark 3.1: The implementation of system's (1) inversion requires system (1) be BIBO stable and invertible (that is, without unstable zero dynamic). When the highest-order derivatives of system input $u^{(m)}$ is solved, the other u related derivatives can be obtained by integration of $u^{(m)}$.

3.2 New U-inverter design

Section 3.1 has explained the basic concept/configuration of the U-control system. Manifestly, the solving process of the controlled plant's inversion (9) requires the system input u and output y and their related high-order derivatives $u^{(m)}$ and $y^{(n)}$. In this section, a new U-inverter design based on the input/output model (1) is presented. The dashed area in Figure 2 shows the basic design framework of this new U-inverter. Where r is the reference input of the U-inverter (marked in dashed zone), u and y_1 are the controlled plant input/output, respectively.

Based on the U-control framework, the U-inverter is designed to convert the controlled plant into an identity matrix or a unit constant. When there are no modelling errors and external disturbance from the system, $G_0^{-1}G_P = 1$. In this case, the input of the U-inverter equals to the output of controlled plant, that is, $r = y_1$.

Let the controlled plant input u be

$$u = k_1(r - y_1) \tag{10}$$

where $k_1 > 0$ is a sufficient large constant. It follows from (10) that

$$\begin{cases} u = k_1(r - y_1) \\ \dot{u} = k_1(\dot{r} - \dot{y}_1) \\ \quad\vdots \\ u^{(n)} = k_1(r^{(n)} - y_1^{(n)}) \end{cases} \tag{11}$$

Clearly, from Equations (10) and (11) and Figure 2, the proposed U-inverter only requires the signal information of system output y_1 and reference r. Different from the general U-inverter, high-order derivatives of y_1 are not required in the whole design procedure. From (11), it follows that

$$\begin{cases} y_1 = r - \dfrac{u}{k_1} \\ \dot{y}_1 = \dot{r} - \dfrac{u}{k_1} \\ \quad\vdots \\ y_1^{(n-1)} = r^{(n-1)} - \dfrac{u^{(n-1)}}{k_1} \\ y_1^{(n)} = r^{(n)} - \dfrac{u^{(n)}}{k_1} \end{cases} \tag{12}$$

From (1),

$$y_1^{(n)} = f(y_1, \dot{y}_1, \ddot{y}_1, \ldots, y_1^{(n-1)})$$

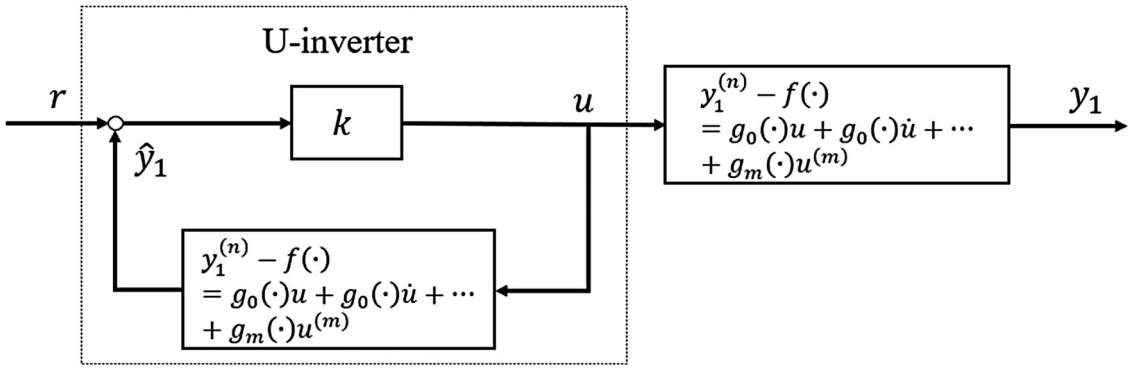

Figure 2. The design framework of new U-inverter.

$$
\begin{aligned}
&+ g_0(y_1, \dot{y}_1, \ddot{y}_1, \ldots, y_1^{(n-1)})u + \ldots \\
&+ g_m(y_1, \dot{y}_1, \ddot{y}_1, \ldots, y_1^{(n-1)})u^{(m)} \\
r^{(n)} - \frac{u^{(n)}}{k_1} &= f\left(r - \frac{u}{k_1}, \dot{r} - \frac{\dot{u}}{k_1}, \ldots, r^{(n-1)} - \frac{u^{(n-1)}}{k_1}\right) \\
&+ g_0\left(r - \frac{u}{k_1}, \dot{r} - \frac{\dot{u}}{k_1}, \ldots, r^{(n-1)} - \frac{u^{(n-1)}}{k_1}\right)u \\
&+ \ldots + g_m\left(r - \frac{u}{k_1}, \dot{r} - \frac{\dot{u}}{k_1}, \right. \\
&\left. \ldots, r^{(n-1)} - \frac{u^{(n-1)}}{k_1}\right)u^{(m)} \qquad (13)
\end{aligned}
$$

Add the same term $f(R) + g_0(R)u + \ldots + g_m(R)u^{(m)}$ to each side of (13) with

$$R = (r, \dot{r}, \ddot{r}, \ldots, r^{(n-1)}) \qquad (14)$$

Then (13) turns to:

$$
\begin{aligned}
&r^{(n)} - \frac{u^{(n)}}{k_1} \\
&= f(R) + g_0(R)u + \ldots + g_m(R)u^{(m)} \\
&+ f\left(r - \frac{u}{k_1}, \dot{r} - \frac{\dot{u}}{k_1}, \ldots, r^{(n-1)} - \frac{u^{(n-1)}}{k_1}\right) \\
&- f(r, \dot{r}, \ldots, r^{(n-1)}) \\
&+ g_0\left(r - \frac{u}{k_1}, \dot{r} - \frac{\dot{u}}{k_1}, \ldots, r^{(n-1)} - \frac{u^{(n-1)}}{k_1}\right)u \\
&- g_0(r, \dot{r}, \ldots, r^{(n-1)})u \\
&+ \ldots + g_m\left(r - \frac{u}{k_1}, \dot{r} - \frac{\dot{u}}{k_1}, \ldots, r^{(n-1)} - \frac{u^{(n-1)}}{k_1}\right)u^{(m)} \\
&- g_m(r, \dot{r}, \ldots, r^{(n-1)})\, u^{(m)} \qquad (15)
\end{aligned}
$$

Because the functions $f(r, \dot{r}, \ldots, r^{(n-1)})$ and $g_i(r, \dot{r}, \ldots, r^{(n-1)}), i \in \mathbb{N}$ are both smooth, the following inequalities exist at least locally

$$
\begin{aligned}
&\left\| f\left(r - \frac{u}{k_1}, \dot{r} - \frac{\dot{u}}{k_1}, \ldots, r^{(n-1)} - \frac{u^{(n-1)}}{k_1}\right) \right. \\
&\left. - f(r, \dot{r}, \ldots, r^{(n-1)}) \right\| \le \gamma_1 \left\| \left(\frac{u}{k_1}, \frac{\dot{u}}{k_1}, \ldots, \frac{u^{(n-1)}}{k_1}\right) \right\| \\
&= \frac{\gamma_1}{k_1} \|(u, \dot{u}, \ldots, u^{(n-1)})\| \qquad (16)
\end{aligned}
$$

And

$$
\begin{aligned}
&\left\| g_i\left(r - \frac{u}{k_1}, \dot{r} - \frac{\dot{u}}{k_1}, \ldots, r^{(n-1)} - \frac{u^{(n-1)}}{k_1}\right) \right. \\
&\left. - g_i(r, \dot{r}, \ldots, r^{(n-1)}) \right\| \le \gamma_2 \left\| \left(\frac{u}{k_1}, \frac{\dot{u}}{k_1}, \ldots, \frac{u^{(n-1)}}{k_1}\right) \right\| \\
&= \frac{\gamma_2}{k_1} \|(u, \dot{u}, \ldots, u^{(n-1)})\| \qquad (17)
\end{aligned}
$$

where γ_1 and γ_2 are Lipschitz constants. For convenient description, let

$$U = ||(u, \dot{u}, \ddot{u}, \ldots, u^{(n-1)})|| \qquad (18)$$

Move term $f(R) + g_0(R)u + \ldots + g_m(R)u^{(m)}$ to the left side of Equation (15), organize it according to principles described in (16) and (17), then Equation (15) turns into

$$
\begin{aligned}
&\left| r^{(n)} - \frac{u^{(n)}}{k_1} - (f(R) + g_0(R)u + \ldots + g_m(R)u^{(m)}) \right| \\
&\le \frac{\gamma_1}{k_1}U + \frac{\gamma_2}{k_1}U|u| + \frac{\gamma_2}{k_1}U|\dot{u}| + \ldots + \frac{\gamma_2}{k_1}U|u^{(m)}| \qquad (19)
\end{aligned}
$$

From (19), it is clearly that when $k_1 \to \infty$, the right side of Equation (19) has

$$\lim_{k_1 \to \infty} \frac{\gamma_1}{k_1}U + \frac{\gamma_2}{k_1}U|u| + \frac{\gamma_2}{k_1}U|\dot{u}| + \ldots + \frac{\gamma_2}{k_1}U|u^{(m)}| = 0 \qquad (20)$$

Therefore, the left side of Equation (19) correspondingly has

$$
\begin{aligned}
&\lim_{k_1 \to \infty} \left| r^{(n)} - \frac{u^{(n)}}{k_1} - (f(R) + g_0(R)u + \ldots + g_m(R)u^{(m)}) \right| \\
&= 0
\end{aligned}
$$

$$\lim_{k_1\to\infty} r^{(n)} - \frac{u^{(n)}}{k_1} = f(R) + g_0(R)u + \ldots + g_m(R)u^{(m)} \quad (21)$$

Let (1) subtract (21), it comes

$$\begin{aligned} y_1^{(n)} - \left(r^{(n)} - \frac{u^{(n)}}{k_1}\right) &= f(Y_1) - f(R) + g_0(Y_1)u - g_0(R)u \\ &\quad + \ldots + g_m(Y_1)u^{(m)} - g_m(R)u^{(m)} \\ &= f(Y_1) - f(R) + (g_0(Y_1) - g_0(R))u + \ldots \\ &\quad + (g_m(Y_1) - g_m(R))u^{(m)} \end{aligned} \quad (22)$$

Since the functions $f(r, \dot{r}, \ldots, r^{(n-1)})$ and $g_i(r, \dot{r}, \ldots, r^{(n-1)})$, $i \in N$ are smooth, the following inequalities exist at least locally

$$\begin{aligned} &||g_i(r, \dot{r}, \ldots, r^{(n-1)}) - g_i(y_1, \dot{y}_1, \ldots, y_1^{(n-1)})|| \\ &\quad \le \gamma_3 ||(r - y_1, \dot{r} - \dot{y}_1, \ldots, r^{(n-1)} - y_1^{(n-1)})|| \\ &\quad = \frac{\gamma_3}{k_1} ||(u, \dot{u}, \ldots, u^{(n-1)})|| \end{aligned} \quad (23)$$

where γ_3 is Lipschitz constant. Move term $f(Y_1) - f(R)$ to the left side of Equation (22), it has

$$\begin{aligned} &\left| y_1^{(n)} - \left(r^{(n)} - \frac{u^{(n)}}{k_1}\right) - (f(Y_1) - f(R)) \right| \\ &\quad \le \frac{\gamma_3}{k_1} U|u| + \frac{\gamma_3}{k_1} U|\dot{u}| + \ldots + \frac{\gamma_3}{k_1} U|u^{(m)}| \\ &\quad = \frac{\gamma_3}{k_1} U(|u| + |\dot{u}| + \ldots + u^{(m)}) \end{aligned} \quad (24)$$

When $k_1 > 0$ tends to infinity, the right term in (24) has

$$\lim_{k_1\to\infty} \frac{\gamma_3}{k_1} U(|u| + |\dot{u}| + \ldots + u^{(m)}) = 0 \quad (25)$$

Substituting (25) into (24), it comes

$$\left| y_1^{(n)} - \left(r^{(n)} - \frac{u^{(n)}}{k_1}\right) - (f(Y_1) - f(R)) \right| = 0 \quad (26)$$

Based on (12),

$$y_1^{(n)} - \left(r^{(n)} - \frac{u^{(n)}}{k_1}\right) = y_1^{(n)} - y_1^{(n)} = 0 \quad (27)$$

Because the term $y_1^{(n)} - \left(r^{(n)} - \frac{u^{(n)}}{k_1}\right)$ equals to 0, it can be concluded from (24) that

$$|f(Y_1) - f(R)| = 0 \quad (28)$$

Substituting (28) into (22), it is clear that the left side of Equation (22) is equal to 0 as well as the term $f(Y_1) - f(R)$, then it comes from (22) that

$$\begin{aligned} &(g_0(Y_1) - g_0(R))u + (g_1(Y_1) - g_1(R))\dot{u} + \ldots \\ &\quad + (g_m(Y_1) - g_m(R))u^{(m)} = 0 \end{aligned} \quad (29)$$

Extend (29) by (11), then it becomes

$$\begin{aligned} &(g_0(Y_1) - g_0(R))u + (g_1(Y_1) - g_1(R))\dot{u} + \ldots \\ &\quad + (g_m(Y_1) - g_m(R))u^{(m)} \\ &= k_1((g_0(Y_1) - g_0(R))(r - y_1) + (g_1(Y_1) - g_1(R))(\dot{r} - \dot{y}_1) \\ &\quad + \ldots + (g_m(Y_1) - g_m(R))(r^{(m)} - y_1^{(m)})) = 0 \end{aligned} \quad (30)$$

Let the error e_1 between the reference r and y_1, that is, $e_1 = r - y_1$. Because constant $k_1 > 0$, it follows (30) that

$$\begin{aligned} &(g_0(Y_1) - g_0(R))e_1 + (g_1(Y_1) - g_1(R))\dot{e}_1 + \ldots \\ &\quad + (g_m(Y_1) - g_m(R))e_1^{(m)} = 0 \end{aligned} \quad (31)$$

From Assumption 2.2, the system (31) is globally asymptotically stable. Accordingly, the error e_1 between the reference r and y_1 approaches zero asymptotically, which implies that y_1 converges to r with a large enough gain k. When $y_1 = r$, the system dynamic inversion implemented, which also means the cancelation of system dynamics and nonlinearities is achieved. Therefore, the structure in Figure 2 can be used to design the U-inverter.

Remark 3.2: From (25) to (31), the error between the reference and system output will converge to zero asymptotically when the parameter k adjusted to infinity. It seems this proposed U-inverter is similar to the high-gain feedback controller, but it is not the case. Generally, the high-gain controller requires system state variables (Krishnamurthy et al., 2003; Ma et al., 2018), and the high-gain controller is designed to achieve desired system control performance, whereas the purpose of the proposed U-inverter is the cancelation of system dynamics and nonlinearity. Additionally, this U-inverter is only a part of the U-control system, which aims to construct an inverse model of the controlled plant. Therefore, the basic idea of the proposed U-inverter is different from the high-gain feedback controller. Any point should be mentioned is that the proposed U-inverter only requires the information of the controlled plant input and output. Kumar and Veerachary (2021) do not require system state variables, but the frequency response, pole-zero locations are selected to design system controller.

According to the U-control system design framework in Section 3.1, the updated U-control system design framework is showed in Figure 3, in where the dashed area shows this new U-controller, which contains both invariant controller G_{c1} and the proposed U-inverter. Clearly, only system output and controller output are required in the system design process.

3.3 DOB design

From Sections 3.1 and 3.2, a new U-controller design is proposed based on this new U-inverter. However, from Figure 3, the model in the U-controller required to be same with the controlled model, that is, the whole U-control system is designed without system internal uncertainties and external disturbances. In practice application, this 'perfect modelling' is hardly existed. Therefore, inspired by (Ding et al., 2019), a nonlinear

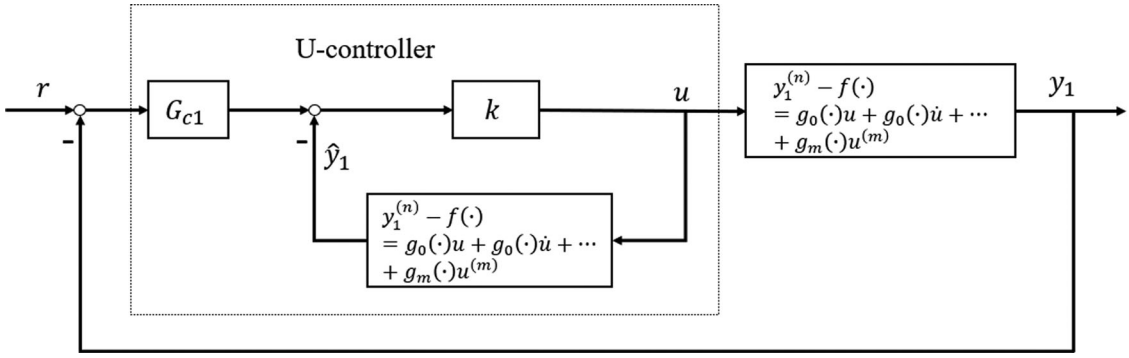

Figure 3. New U-control system design framework.

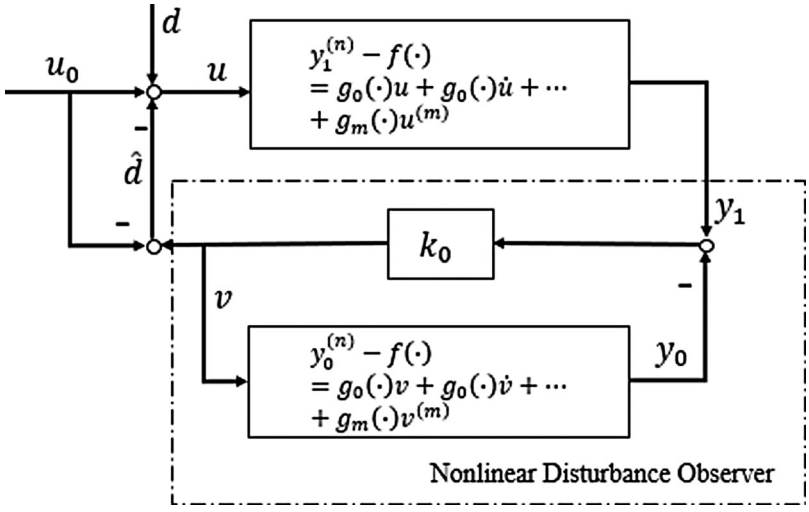

Figure 4. The framework of nonlinear DOB.

input/output model-based DOB is introduced in the U-control system design, which also only requires the information of system input and output. The framework of NDOB in Ding et al. (2019) is shown in Figure 4.

Set the nominal model of system (1) as follows for NDOB design:

$$y_0^{(n)} = f(Y_0) + g_0(Y_0)v + \ldots + g_m(Y_0)v^{(m)},\ m \le n \tag{32}$$

where y_0 and v are the observer system output and input, respectively, $f(Y_0)$ and $g_i(Y_0)$ are smooth function associated with

$$Y_0 = \left(y_0, \dot{y}_0, \ddot{y}_0, \ldots, y_0^{(n-1)}\right)$$

Let the input of nominal modelled system (32) be

$$v = k_0(y_1 - y_0) \tag{33}$$

where y_1 is the practice system output and k_0 is a large constant. Thus, the disturbance d and other modelling uncertainties can be observed as $\hat{d} = v - u_0$.

It follows from (33) that

$$\begin{cases} v = k_0(y_1 - y_1) \\ \dot{v} = k_0(\dot{y}_1 - \dot{y}_0) \\ \vdots \\ v^{(n)} = k_0(y_1^{(n)} - y_0^{(n)}) \end{cases} \tag{34}$$

where $k_0 > 0$ is a sufficient large constant, from (34), it follows that,

$$\begin{cases} y_0 = y_1 - \dfrac{v}{k_0} \\ \dot{y}_0 = \dot{y}_1 - \dfrac{\dot{v}}{k_0} \\ \vdots \\ y_0^{(n-1)} = {y_1}^{(n-1)} - \dfrac{v^{(n-1)}}{k_0} \\ y_0^{(n)} = {y_1}^{(n)} - \dfrac{v^{(n)}}{k_0} \end{cases} \tag{35}$$

Then substituting (35) into (32), it comes

$$\begin{aligned} &{y_1}^{(n)} - \frac{v^{(n)}}{k_0} \\ &= f\left(y_1 - \frac{v}{k_0}, \dot{y}_1 - \frac{\dot{v}}{k_0}, \ldots, {y_1}^{(n-1)} - \frac{v^{(n-1)}}{k_0}\right) \\ &\quad + g_0\left(y_1 - \frac{v}{k_0}, \dot{y}_1 - \frac{\dot{v}}{k_0}, \ldots, {y_1}^{(n-1)} - \frac{v^{(n-1)}}{k_0}\right)v \end{aligned}$$

$$+\ldots+g_m\left(y_1-\frac{v}{k_0},\dot{y}_1-\frac{\dot{v}}{k_0},\ldots,{y_1}^{(n-1)}-\frac{v^{(n-1)}}{k_0}\right)v^{(m)} \tag{36}$$

Add the same term $f(Y_1)+g_0(Y_1)v+\ldots+g_m(Y_1)v^{(m)}$ to each side of Equation (36), then it becomes

$$\begin{aligned}{y_1}^{(n)}=&\frac{v^{(n)}}{k_0}+f(Y_1)+g_0(Y_1)v+\ldots+g_m(Y_1)v^{(m)}\\&+\left(f\left(y_1-\frac{v}{k_0},\dot{y}_1-\frac{\dot{v}}{k_0},\ldots,{y_1}^{(n-1)}-\frac{v^{(n-1)}}{k_0}\right)\right.\\&\left.-f(y_1,\dot{y}_1,\ldots,y_1^{(n-1)})\right)\\&+\left(g_0\left(y_1-\frac{v}{k_0},\dot{y}_1-\frac{\dot{v}}{k_0},\ldots,{y_1}^{(n-1)}-\frac{v^{(n-1)}}{k_0}\right)\right.\\&\left.-g_0(y_1,\dot{y}_1,\ldots,y_1^{(n-1)})\right)v\\&+\ldots+\left(g_m\left(y_1-\frac{v}{k_0},\dot{y}_1-\frac{\dot{v}}{k_0},\ldots,{y_1}^{(n-1)}\right.\right.\\&\left.\left.-\frac{v^{(n-1)}}{k_0}\right)-g_m(y_1,\dot{y}_1,\ldots,y_1^{(n-1)})\right)v^{(m)}\end{aligned} \tag{37}$$

Because the functions $f(r,\dot{r},\ldots,r^{(n-1)})$ and $g_i(r,\dot{r},\ldots,r^{(n-1)})$, $i\in N$ are smooth, the following inequalities exist at least locally

$$\begin{aligned}&\left\|f\left(y_1-\frac{v}{k_0},\dot{y}_1-\frac{\dot{v}}{k_0},\ldots,{y_1}^{(n-1)}-\frac{v^{(n-1)}}{k_0}\right)\right.\\&\quad\left.-f(y_1,\dot{y}_1,\ldots,y_1^{(n-1)})\right\|\le\gamma_4\left\|\left(\frac{v}{k_0},\frac{\dot{v}}{k_0},\ldots,\frac{v^{(n-1)}}{k_0}\right)\right\|\\&=\frac{\gamma_4}{k_0}||(v,\dot{v},\ldots,v^{(n-1)})||\end{aligned} \tag{38}$$

And

$$\begin{aligned}&\left\|g_i\left(y_1-\frac{v}{k_0},\dot{y}_1-\frac{\dot{v}}{k_0},\ldots,{y_1}^{(n-1)}-\frac{v^{(n-1)}}{k_0}\right)\right.\\&\quad\left.-g_i(y_1,\dot{y}_1,\ldots,y_1^{(n-1)})\right\|\le\gamma_5\left\|\left(\frac{v}{k_0},\frac{\dot{v}}{k_0},\ldots,\frac{v^{(n-1)}}{k_0}\right)\right\|\\&=\frac{\gamma_5}{k_0}||(v,\dot{v},\ldots,v^{(n-1)})||\end{aligned} \tag{39}$$

where γ_4 and γ_5 are Lipschitz constants. Then move term $f(Y_1)+g_0(Y_1)v+\ldots+g_m(Y_1)v^{(m)}$ to the left side of Equation (37), organize it according to principles described in (38) and (39), then Equation (37) can be turned into

$$\begin{aligned}&|{y_1}^{(n)}-(f(Y_1)+g_0(Y_1)v+\ldots+g_m(Y_1)v^{(m)})|\\&\le\frac{v^{(n)}}{k_0}+\frac{\gamma_4}{k_0}H+\frac{\gamma_5}{k_0}H(|v|+|\dot{v}|+\ldots+v^{(m)})\end{aligned} \tag{40}$$

When k_0 goes infinite, the right side of Equation (40) has

$$\lim_{k_0\to\infty}\frac{v^{(n)}}{k_0}+\frac{\gamma_4}{k_0}H+\frac{\gamma_5}{k_0}H(|v|+|\dot{v}|+\ldots+v^{(m)})=0 \tag{41}$$

Therefore, the left side of Equation (40) turns into

$$\begin{aligned}&|{y_1}^{(n)}-(f(Y_1)+g_0(Y_1)v+\ldots+g_m(Y_1)v^{(m)})|=0\\&{y_1}^{(n)}=f(Y_1)+g_0(Y_1)v+\ldots+g_m(Y_1)v^{(m)}\end{aligned} \tag{42}$$

Combining (42) and (1), it gives

$$\begin{aligned}{y_1}^{(n)}-{y_1}^{(n)}=&f(Y_1)+g_0(Y_1)u+\ldots+g_m(Y_1)u^{(m)}\\&-(f(Y_1)+g_0(Y_1)v+\ldots+g_m(Y_1)v^{(m)})\\=&g_0(Y_1)(v-u)+g_1(Y_1)(\dot{v}-\dot{u})+\ldots\\&+g_m(Y_1)(v^{(m)}-u^{(m)})\end{aligned} \tag{43}$$

It is clear that the left side of Equation (43) equals to 0, let the error e_2 be $e_2=v-u$, it comes from (43) that

$$g_0(Y_1)e_2+g_1(Y_1)\dot{e}_2+\ldots+g_m(Y_1)e_2^{(m)}=0 \tag{44}$$

From Assumption 2.2, system (44) is globally asymptotically stable. Accordingly, the error between u and v approaches zero asymptotically. Therefore, the observed $\hat{d}$ can converge to the lumped disturbance represented by the practical disturbance d and modelling uncertainties asymptotically.

3.4 DOBUC design

The proposed U-control in 3.2 shows the efficient control design which only requires the system output, however, this efficiency strictly appears in the case of model matched. In practice, the modelling errors and system external noise will exist and restrict the proposed U-control performance. The input/output model-based DOB described in 3.3 presented its main advantages in observing the system disturbances with only system input/output information. This DOB can amalgamate all uncertainties and system disturbances into system input channel, which will make disturbance compensation be implemented easily. Accordingly, the combination of this nonlinear DOB and the proposed U-control makes it possible to reduce U-control's sensitivity and improve the robustness of the control system.

Based on the new U-control system design framework in 3.2 and DOB described in 3.3, this study proposed a new DOBUC design framework shown in Figure 5. Concretely, this DOBUC has three loops: DOB in the inner loop can estimate the disturbance caused by modelling errors and system noises, and then amalgamate them into the system input channel; the U-inverter in the inner loop will cancel both the system dynamics and nonlinearity, convert the controlled plant to an identity matrix or unit constant when combined with its dynamic inversion; G_{c1} in the outer loop is used to design the desired control performance. Manifestly, if the control system is perfect modelled and free of system external disturbance, the inner DOB will not be activated and the system will be converted into a simple linear closed-loop feedback control system with the dynamic cancelation from the U-inverter; when disturbance exists in system,

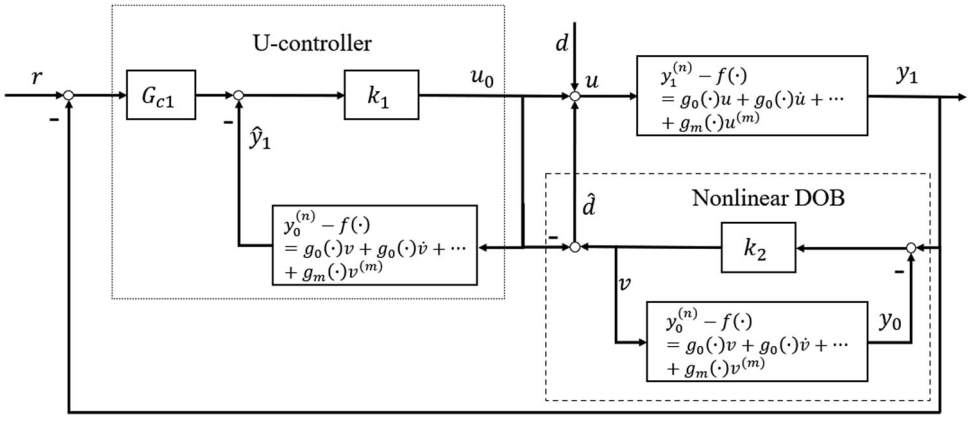

Figure 5. New DOB-based U-control design framework.

the U-controller will compensate the disturbance estimated by activated DOB into the input channel. Finally, the framework of DOBUC is equivalent to the followed framework (Figure 6):

Accordingly, the design procedures for the proposed DOBUC are:

(1) Design the U-inverter based on Section 3.2. The design parameter k_1 should be selected large enough to satisfy (20) to implement an efficient U-inverter. It should be mentioned that the model inversion should exist and satisfy the Lipschitz continuity with globally uniformly:

$$||G(x_1) - G(x_2)|| \leq \gamma_1 ||Gx_1 - x_2||, \quad \forall x_1, x_2 \in \mathbb{R}^n$$
$$||G^{-1}(x_1) - G^{-1}(x_2)|| \leq \gamma_2 ||G^{-1}x_1 - x_2||, \quad \forall x_1, x_2 \in \mathbb{R}^n$$

(2) Design the nonlinear DOB based on Section 3.3. The design parameter k_0 should be large enough to satisfy (41) and guarantee that the disturbance estimation error can converge to a small region.

(3) Design invariant controller G_{c1} with customer defined damping ratio ζ and undamped natural frequency ω_n to achieve control performance specifications. Where $G_{c1} = \frac{G}{1-G}$ and $G = \frac{{\omega_n}^2}{s^2+2\zeta\omega_n s+{\omega_n}^2}$.

Remark 3.3: Theoretically, the larger parameters k_0, k_1 can realise more efficient u-inverter and improved disturbance estimation performance. However, the system output noise level will also be increased by the increasing value of k_0 and k_1. Accordingly, the parameters k_0 and k_1 should be adjusted from small to large until the control performance specifications are meted. It also should be noticed that k_1 need to be larger than k_0 to ensure the U-inverter converges faster than the nonlinear DOB because this DOB requires the information from U-controller's output to estimate the disturbance.

4. Experimental simulation

Compared with the traditional fossil fuels, renewable energy has become popular in recent decades. In the situation of growing global energy demand while significantly reducing reliance on fossil-fuels, environmentally friendly wind energy received wide concertation (Ahmad et al., 2020). According to the Global Wind Energy Statistics 2020 (Global Wind Energy Council, 2021), China accounted for 36.42% (237 029 MW) of the world's installed wind power capacity and the United States accounted for 16.20% (105 433 MW). In WECS, variable-speed wind turbines (VSWT) convert wind energy into electricity. Therefore, an efficient VSWT control strategy will exploit maximum power generation and improve the power quality (Wang et al., 2011). The latest advanced control articles (de Siqueira & Peng, 2021; Ghaffarzadeh & Mehrizi-Sani, 2020; Milev et al., 2020) mainly focus on solving the complex nonlinear dynamics and difficulty measuring speed of WECS in real-time applications. Paper (Li et al., 2020) firstly applied U-control method on WECS, although it did not consider modelling errors and disturbances such as unmeasurable wind speed, the implementation of its complex nonlinear dynamics and good control performance are still worthy for further study.

4.1 Modelling of WECS

The aerodynamic torque of the turbine is:

$$T_a = \frac{1}{2}\rho\pi R^3 C_q(\lambda, \beta)(\hat{v} - \xi)^2 \tag{45}$$

where ρ and R are the air density and the length of the rotor blade; $\hat{v}$ and ξ are the effective wind velocity estimate and practical measurement disturbance; $C_q(\lambda, \beta)$ is the wind turbine power conversion efficiency coefficient, which depends on the tip-speed ratio λ and blade pitch angle β:

$$C_q(\lambda, \beta) = \frac{0.22}{\lambda}\left(\frac{116}{m} - 0.4\beta - 5\right) exp(-12.5/m) \tag{46}$$

With

$$\frac{1}{m} = \frac{1}{\lambda + 0.08\beta} - \frac{0.035}{\beta^3 + 1} \tag{47}$$

The tip-speed ratio λ is defined as

$$\lambda = \frac{R\omega_r}{v} \tag{48}$$

where ω_r is the rotor angular speed. Therefore, the rotor power P_a captured by the wind turbine is the product of the aerodynamic torque and blade speed, which donated from (22)

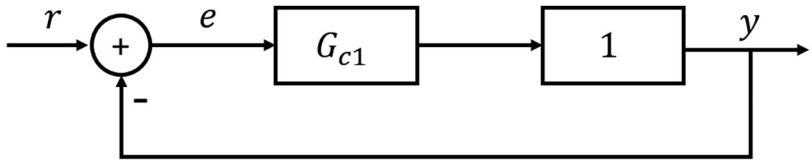

Figure 6. Equivalent U-control framework after NDOB compensation.

as

$$P_a = \omega_r T_a = \frac{1}{2}\rho\pi R^2 C_p(\lambda,\beta)(\hat{v}-\xi)^3 \tag{49}$$

With

$$C_p(\lambda,\beta) = C_q(\lambda,\beta)\lambda \tag{50}$$

According to the drive train scheme in Figure 7, the dynamics of rotor speed ω_r and generator speed ω_g are driven by the rotor torque T_a, the low-speed torque T_{ls}, the high-speed torque T_{hs} and the electromagnetic torque T_{em}:

$$\begin{cases} J_r\dot{\omega}_r = T_a - K_r\omega_r - T_{ls} \\ J_g\dot{\omega}_g = T_{hs} - K_g\omega_g - T_{em} \end{cases} \tag{51}$$

where J_r and K_r, J_g and K_g are inertia and external damping for rotor and generator, respectively. The conversion rate between ω_r and ω_g can be described by gearbox ratio n_g as

$$n_g = \frac{\omega_g}{\omega_r} = \frac{T_{ls}}{T_{hs}} \tag{52}$$

Invoking (52), it comes from the generator dynamic in (51):

$$n_g{}^2 J_g\dot{\omega}_r = T_{ls} - n_g{}^2 K_g\omega_r - n_g T_{em} \tag{53}$$

Thus, the drive train model comes from the combination of (51) with (53),

$$J_t\dot{\omega}_r = T_a - K_t\omega_r - T_g \tag{54}$$

where

$$\begin{cases} J_t = J_r + n_g^2 J_g \\ K_t = K_r + n_g^2 K_g \\ T_g = n_g T_{em} \end{cases} \tag{55}$$

Then, the system output is expressed as

$$P_g = T_g\omega_r \tag{56}$$

System (54) describes the relationship between system input and output. Substituting (56) into (54), the drive train model will be:

$$\begin{aligned} J_t\left(\frac{\dot{P}_g}{T_g}\right) &= T_a - K_t\frac{P_g}{T_g} - T_g \\ \left(\frac{\dot{P}_g T_g - P_g\dot{T}_g}{T_g{}^2}\right) &= \frac{T_a}{J_t} - \frac{K_t}{J_t}\frac{P_g}{T_g} - \frac{1}{J_t}T_g \\ \dot{P}_g T_g - P_g\dot{T}_g &= \frac{1}{J_t}T_a T_g{}^2 - \frac{K_t}{J_t}P_g T_g - \frac{1}{J_t}T_g{}^3 \end{aligned} \tag{57}$$

Table 1. Wind turbine parameters.

Rated power	1.5 MW
Rotor radius	$R = 38.5$ m
Rotor inertia	$J_r = 4{,}456{,}761$ kg.m^2
Generator inertia	$J_g = 123$ kg.m^2
Rotor friction coefficient	$K_r = 45.52$ N.m/rad/s
Generator friction coefficient	$K_g = 0.4$ N.m/rad/s
Gearbox ratio	$n_g = 104.494$
Air density	$\rho = 1.12$

The description in (57) shows the modelling of WECS. Let the generator torque T_g and generator power P_g be control input u and output y, respectively, it has:

$$\dot{y}u - y\dot{u} = \frac{1}{J_t}T_a u^2 - \frac{K_t}{J_t}yu - \frac{1}{J_t}u^3 \tag{58}$$

Convert (58) into its U- realization:

$$\begin{cases} \dot{y} = \lambda_0 f_0(\dot{u}) + \lambda_1 f_1(\dot{u}) \\ \lambda_0 \quad = \frac{1}{J_t}T_a u - \frac{K_t}{J_t}y - \frac{1}{J_t}u^2, f_0(\dot{u}) = 1 \\ \lambda_1 = \frac{y}{u}, f_1(\dot{u}) = \dot{u} \end{cases} \tag{59}$$

4.2 Simulation results

The related parameters in WECS modelling are provided in Table 1 (Meng et al., 2013).

The ratio of desired power P_d and ideal maximum power P_{amax} is $n_p = 0.8$. Therefore, the parameters in (59) are:

$$\begin{cases} J_t = J_r + n_g^2 J_g = 5.7998 \times 10^6 \\ K_t = K_r + n_g^2 K_g = 4.4131 \times 10^3 \\ \frac{K_t}{J_t} = 7.609 \times 10^{-4} \end{cases} \tag{60}$$

The turbulence intensity is 10% and the mean value of wind speed v in this experiment is 9 m/s (Meng et al., 2013). This simulation experiment introduces the wind speed sensor error because of its inevitably disturbances. Accordingly, the speed sensor error is chosen as a 10 Hz white noise, with the value from −0.5 to 0.5. Figure 8 shows the wind speed with and without sensor error.

The block framework of this control system is given in Figure 9.

According to the design framework presented in Section 3.4, the parameter in U-inverter is: $k_1 = 1000$ and in nonlinear observer is $k_2 = 500$. To assure a fast-tracking performance without overshooting, the damping ratio and undamped natural frequency are chosen as $\zeta = 1$ and $\omega_n = 10$ for invariant

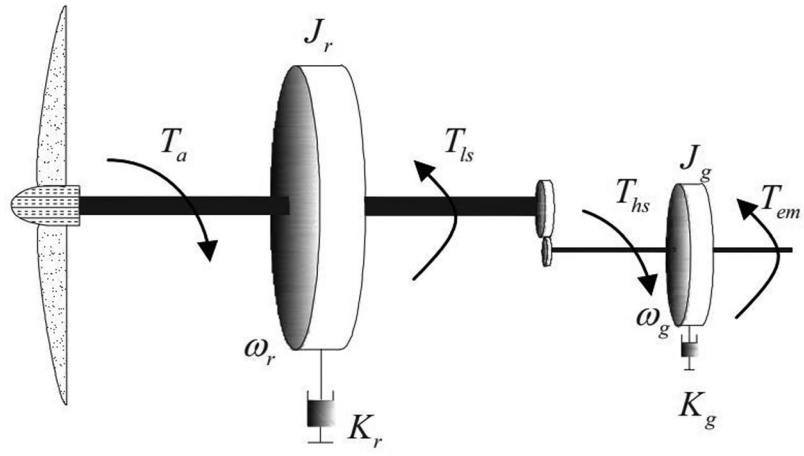

Figure 7. Schematic diagram of drive train.

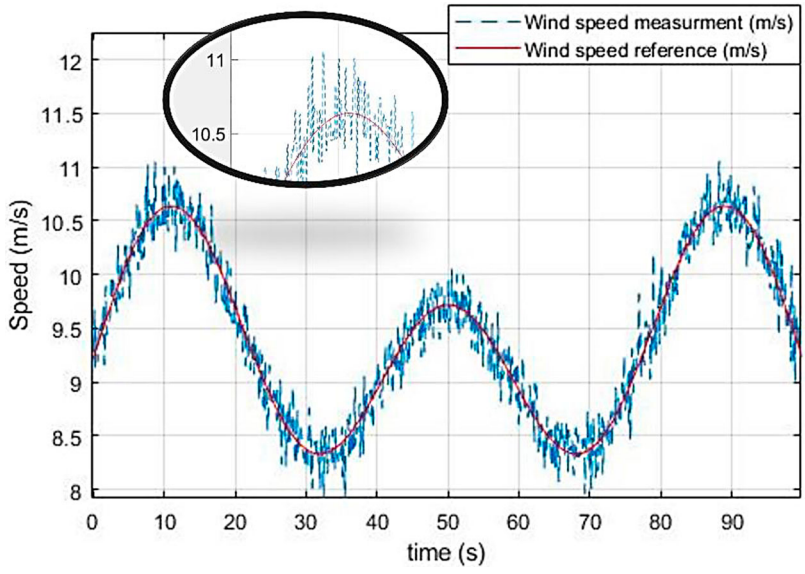

Figure 8. Wind speed measurement.

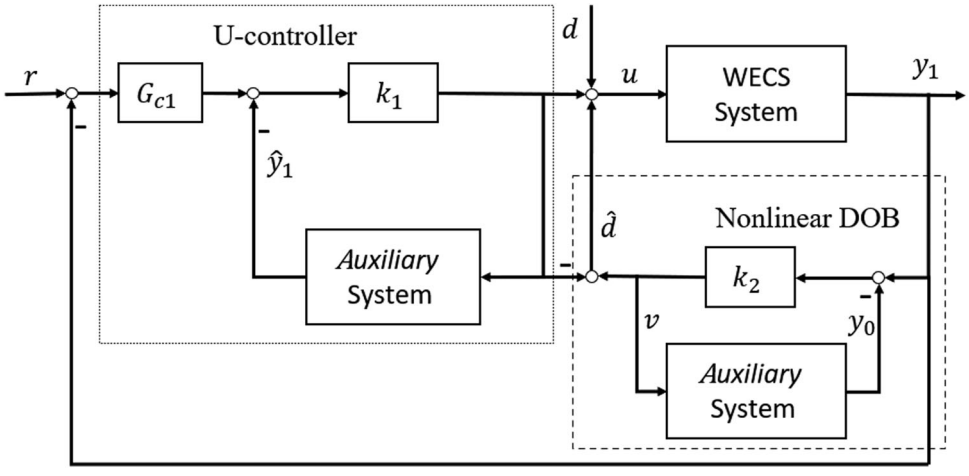

Figure 9. Block framework of WECS with UDOBC.

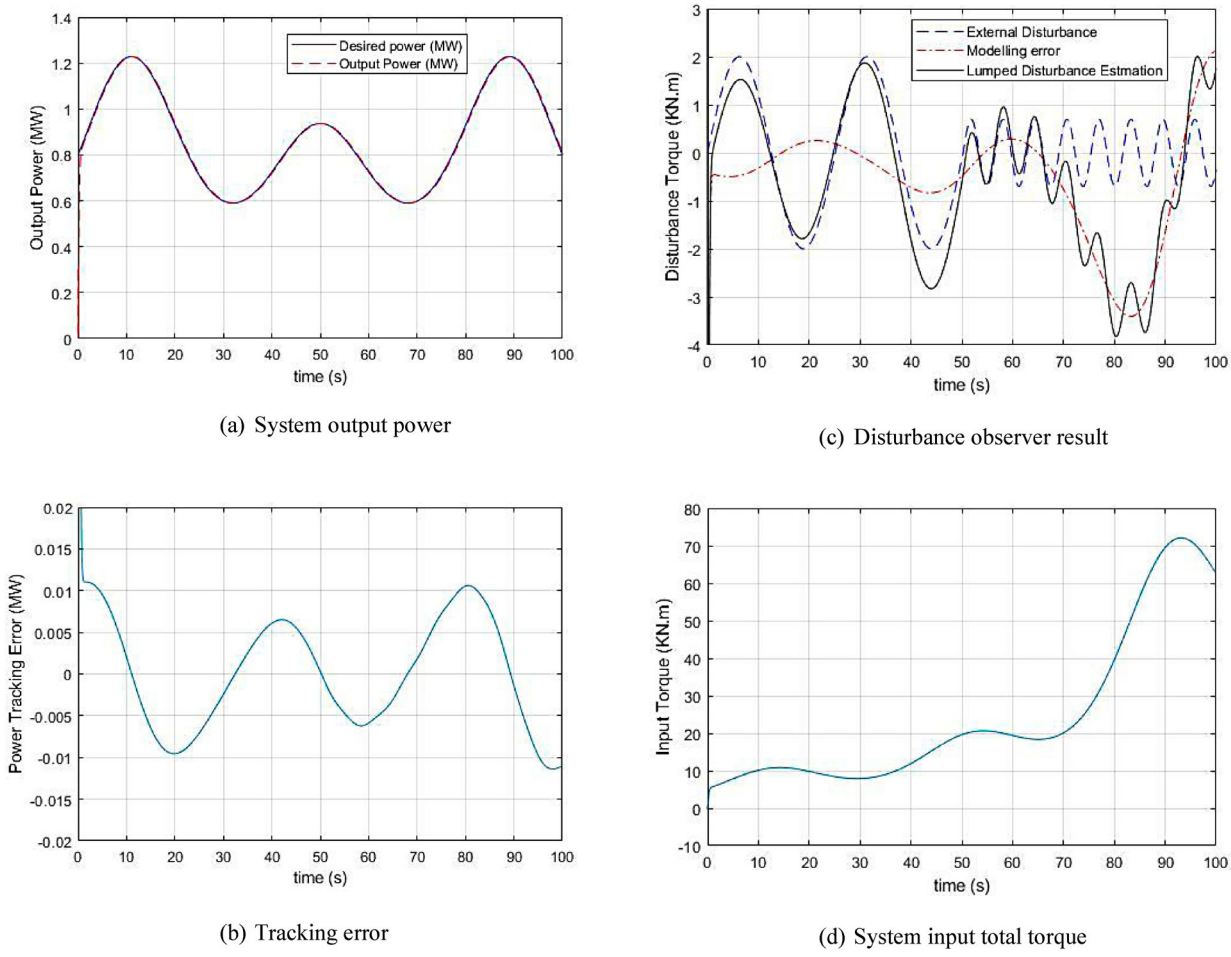

(a) System output power

(c) Disturbance observer result

(b) Tracking error

(d) System input total torque

Figure 10. Simulation results of WECS.

controller design:

$$G_{c1} = \frac{1}{0.01s^2 + 0.2s}$$

Assume the disturbance d is defined as:

$$d = \begin{cases} 2\sin\left(\frac{t}{4}\right) & 0 \le t < 16\pi \\ 0.7\sin(t) & 16\pi \le t < 100 \end{cases}$$

Additionally, modelling errors are considered in this experiment simulation with $\Delta J_t = -0.9J_t$, $\Delta K_t = 2K_t$ and $\Delta T_a = 4T_a$. Therefore, WECS (57) changed to:

$$\dot{P}_g T_g - P_g \dot{T}_g = \frac{5T_a}{0.1J_t} {T_g}^2 - \frac{3K_t}{J_t} P_g T_g - \frac{1}{0.2J_t} {T_g}^3 \qquad (61)$$

The simulation results can be observed from Figure 10. From Figure 10(a), the proposed DOBUC method has good tracking performance; the tracking error rate is less than 1% (compared to peak output power) from Figure 10(b). Obviously, the NDOB shows efficacy in observation of both system disturbance and modelling errors from Figure 10(c) and the controller output is smooth without chattering from Figure 10(d).

5. Conclusions

This study proposes a novel DOBUC framework for linear/nonlinear systems. It removes the restriction on the current state feedback U-control systems that request the state variables observable or measurable. The proposed U-inverter provides a robust dynamic inversion of the control plant, so that it makes the U-control inherit the robustness throughout the control system operation. It should be noted that this DOBUC requires the controlled input/output system being minimum-phase or stable zero dynamic in more general terms, which should take care in applications. Future study topics could be those expanding the proposed framework to MIMO systems and taking up bench tests of practical systems.

Acknowledgements

The authors express their gratitude to the editors and the anonymous reviewers for their helpful comments and constructive suggestions with regard to the revision of the paper. The first author is acknowledging the partial PhD studentship for the research project.

Disclosure statement

No potential conflict of interest was reported by the author(s).

Data availability statement

The data used to support the findings of this study are available from the corresponding author upon request.

References

Ahmad, T., Zhang, H., & Yan, B. (2020). A review on renewable energy and electricity requirement forecasting models for smart grid and buildings. *Sustainable Cities and Society*, *55*, Article 102052. https://doi.org/10.1016/j.scs.2020.102052

Ahmed, N., Chen, M., & Shao, S. (2020). Disturbance observer based tracking control of quadrotor with high-order disturbances. *IEEE Access*, *8*, 8300–8313. https://doi.org/10.1109/ACCESS.2020.2964013

Chen, J., Sun, R., & Zhu, B. (2020). Disturbance observer-based control for small nonlinear UAV systems with transient performance constraint. *Aerospace Science and Technology*, *105*, Article 106028. https://doi.org/10.1016/j.ast.2020.106028

Chen, W. H. (2003). Nonlinear disturbance observer-enhanced dynamic inversion control of missiles. *Journal of Guidance, Control, and Dynamics*, *26*(1), 161–166. https://doi.org/10.2514/2.5027

Chen, W. H., Ballance, D. J., Gawthrop, P. J., & O'Reilly, J. (2000). A nonlinear disturbance observer for robotic manipulators. *IEEE Transactions on Industrial Electronics*, *47*(4), 932–938. https://doi.org/10.1109/41.857974

Chen, W. H., Yang, J., Guo, L., & Li, S. (2016). Disturbance-observer-based control and related methods—An overview. *IEEE Transactions on Industrial Electronics*, *63*(2), 1083–1095. https://doi.org/10.1109/TIE.2015.2478397

Conte, G., Moog, C. H., & Perdon, A. M. (2007). *Algebraic methods for nonlinear control systems*. Springer Science & Business Media.

de Siqueira, L. M. S., & Peng, W. (2021). Control strategy to smooth wind power output using battery energy storage system: A review. *Journal of Energy Storage*, *35*, Article 102252. https://doi.org/10.1016/j.est.2021.102252

Ding, S., Chen, W. H., Mei, K., & Murray-Smith, D. J. (2019). Disturbance observer design for nonlinear systems represented by input–output models. *IEEE Transactions on Industrial Electronics*, *67*(2), 1222–1232. https://doi.org/10.1109/TIE.2019.2898585

Ding, S., Park, J. H., & Chen, C. C. (2020). Second-order sliding mode controller design with output constraint. *Automatica*, *112*, Article 108704. https://doi.org/10.1016/j.automatica.2019.108704

Ghaffarzadeh, H., & Mehrizi-Sani, A. (2020). Review of control techniques for wind energy systems. *Energies*, *13*(24), Article 6666. https://doi.org/10.3390/en13246666

Global Wind Energy Council. (2021). *Global wind report2021*.

Hussain, N. A. A., Ali, S. S. A., Ovinis, M., Arshad, M. R., & Al-Saggaf, U. M. (2019). Underactuated coupled nonlinear adaptive control synthesis using U-model for multivariable unmanned marine robotics. *IEEE Access*, *8*, 1851–1865. https://doi.org/10.1109/ACCESS.2019.2961700

Krishnamurthy, P., Khorrami, F., & Chandra, R. S. (2003). Global high-gain-based observer and backstepping controller for generalized output-feedback canonical form. *IEEE Transactions on Automatic Control*, *48*(12), 2277–2283. https://doi.org/10.1109/TAC.2003.820226

Kumar, N., & Veerachary, M. (2021). Stability region based robust controller design for high-gain boost DC–DC converter. *IEEE Transactions on Industrial Electronics*, *68*(3), 2246–2256. https://doi.org/10.1109/TIE.2020.2972448

Li, R., Zhu, Q., Kiely, J., & Zhang, W. (2020). Algorithms for U-model-based dynamic inversion (UM-dynamic inversion) for continuous time control systems. *Complexity*, *2020*, 1–14. https://doi.org/10.1155/2020/3640210

Li, R., Zhu, Q., Narayan, P., Yue, A., Yao, Y., & Deng, M. (2021). U-model-based two-degree-of-freedom internal model control of nonlinear dynamic systems. *Entropy*, *23*(2), Article 169. https://doi.org/10.3390/e23020169

Li, R., Zhu, Q., Yang, J., Narayan, P., & Yue, X. (2021). Disturbance-Observer-Based U-control (DOBUC) for nonlinear dynamic systems. *Entropy*, *23*(12), Article 1625. https://doi.org/10.3390/e23121625

Ma, T., Liu, Y., Shih, C., & Cao, C. (2018). Handling of nonlinear systems using filtered high-gain output feedback controller. *International Journal of Robust and Nonlinear Control*, *28*(18), 6070–6086. https://doi.org/10.1002/rnc.4360

Meng, W., Yang, Q., Ying, Y., Sun, Y., Yang, Z., & Sun, Y. (2013). Adaptive power capture control of variable-speed wind energy conversion systems with guaranteed transient and steady-state performance. *IEEE Transactions on Energy Conversion*, *28*(3), 716–725. https://doi.org/10.1109/TEC.2013.2273357

Milev, K., Yaramasu, V., Dekka, A., & Kouro, S. (2020, February). Modulated predictive current control of PMSG-based wind energy systems. In *2020 11th power electronics, drive systems, and technologies conference (PEDSTC)* (pp. 1–6). IEEE. https://doi.org/10.1109/PEDSTC49159.2020.9088365

Müller, D., Veil, C., & Sawodny, O. (2020). Disturbance observer based control for quasi continuum manipulators. *IFAC-PapersOnLine*, *53*(2), 9808–9813. https://doi.org/10.1016/j.ifacol.2020.12.2681

Ohishi, K., Nakao, M., Ohnishi, K., & Miyachi, K. (1987). Microprocessor-controlled DC motor for load-insensitive position servo system. *IEEE Transactions on Industrial Electronics*, *IE-34*(1), 44–49. https://doi.org/10.1109/TIE.1987.350923

Shen, H., Li, F., Xu, S., & Sreeram, V. (2018). Slow state variables feedback stabilization for semi-Markov jump systems with singular perturbations. *IEEE Transactions on Automatic Control*, *63*(8), 2709–2714. https://doi.org/10.1109/TAC.2017.2774006

Wang, H., Nayar, C., Su, J., & Ding, M. (2011). Control and interfacing of a grid-connected small-scale wind turbine generator. *IEEE Transactions on Energy Conversion*, *26*(2), 428–434. https://doi.org/10.1109/TEC.2011.2116792

Wang, J., Yang, C., Xia, J., Wu, Z. G., & Shen, H. (2022). Observer-based sliding mode control for networked fuzzy singularly perturbed systems under weighted try-once-discard protocol. *IEEE Transactions on Fuzzy Systems*, *30*(6), 1889. https://doi.org/10.1109/TFUZZ.2021.3070125

Zhang, C., Yan, Y., Wen, C., Yang, J., & Yu, H. (2018). A non-smooth composite control design framework for nonlinear systems with mismatched disturbances: Algorithms and experimental tests. *IEEE Transactions on Industrial Electronics*, *65*(11), 8828–8839. https://doi.org/10.1109/TIE.2018.2811383

Zhang, W., Zhu, Q., Mobayen, S., Yan, H., Qiu, J., & Narayan, P. (2020). U-Model and U-control methodology for nonlinear dynamic systems. *Complexity*, *2020*, 1–13. https://doi.org/10.1155/2020/1050254

Zhu, Q. (2021). Complete model-free sliding mode control (CMFSMC). *Scientific Reports*, *11*(1), 1–15.

Zhu, Q., Li, R., & Yan, X. (2022). U-model-based double sliding mode control (UDSM-control) of nonlinear dynamic systems. *International Journal of Systems Science*, *53*(6), 1153–1169. https://doi.org/10.1080/00207721.2021.1991503

Zhu, Q., Wang, Y., Zhao, D., Li, S., & Billings, S. A. (2015). Review of rational (total) nonlinear dynamic system modelling, identification, and control. *International Journal of Systems Science*, *46*(12), 2122–2133. https://doi.org/10.1080/00207721.2013.849774

Zhu, Q., Zhang, W., Na, J., & Sun, B. (2019, July 27–30). *U-model based control design framework for continuous-time systems*. 2019 Chinese control conference (CCC) (pp. 106–111), Guangzhou, China. https://doi.org/10.23919/ChiCC.2019.8866624

Zhu, Q., Zhang, W., Zhang, J., & Sun, B. (2019). U-neural network-enhanced control of nonlinear dynamic systems. *Neurocomputing*, *352*, 12–21. https://doi.org/10.1016/j.neucom.2019.04.008

Zhu, Q. M., & Guo, L. Z. (2002). A pole placement controller for non-linear dynamic plants. *Proceedings of the Institution of Mechanical Engineers, Part I: Journal of Systems and Control Engineering*, *216*(6), 467–476. https://doi.org/10.1177/095965180221600603